Magnetic Ordering and Anisotropy in Heavy Atom Radicals

Stephen M. Winter,[†] Stephen Hill,[‡] and Richard T. Oakley*,[†]

[†]Department of Chemistry, University of Waterloo, Waterloo, Ontario N2L 3G1 Canada

[‡]National High Magnetic Field Laboratory and Department of Physics, Florida State University, Tallahassee, Florida 32310, United States

ABSTRACT: Recent developments in stable radical chemistry have afforded "heavy atom" radicals, neutral open-shell ($S = 1/2$) molecular species containing heavy p-block elements (S, Se), which display solid-state magnetic properties once considered exclusive to conventional metal-based magnets. These highly spin-delocalized radicals do not associate in the solid state and yet display extensive networks of close intermolecular interactions. Spin density on the heavy atoms allows for increased isotropic and spin−orbit mediated anisotropic exchange effects. Structural variations induced by chemical modification and physical pressure, coupled with ab-initio methods to estimate exchange energies, have facilitated the development of predictive structure/property relationships. These results, coupled with detailed theoretical analyses and magnetic resonance spectroscopic measurements, have provided insight into the magnetic structure of ferromagnetic and spin-canted antiferromagnetic ordered materials as well as an understanding of the importance of spin−orbit coupling contributions to magnetic hysteresis and anisotropy. Isotropic and anisotropic ferromagnetic exchange can also be enhanced indirectly by the incorporation of heavy atoms into nonspin-bearing sites, where they can contribute to multi-orbital spin−orbit coupling.

Figure 1. Alignment of spins associated with magnetic ordering in (a) a bulk ferromagnet (B-FM), (b) a bulk antiferromagnet (B-AFM) and (c) a spin-canted antiferromagnet (SC-AFM).

Chart 1

INTRODUCTION

Interest in magnetic materials, particularly those displaying magnetization associated with the ordering of unpaired electron spins, has a long history.[1] In his 1928 treatise on the origins of ferromagnetism, Heisenberg considered the origins of bulk ferromagnetic (B-FM) order, in which spins on separate sites are aligned in parallel (Figure 1a), and concluded that the presence of atoms with principal quantum number (PQN) ≥ 3 was critical to achieve intersite magnetic exchange interactions sufficiently large to compete with thermal energies ($>kT$).[2] Consistently, the design of ferromagnetic materials is, to this day, based largely on the use of d- and f-block elements and their compounds. In the light of Heisenberg's comments, reports in the early 1990s of B-FM order in crystals of the nitronyl nitroxide **1**[3] and the bisnitroxyl **2**[4] (Chart 1), both neutral organic radicals with one unpaired electron ($S = 1/2$) per nitroxyl, were greeted with some surprise. Despite their low ordering (Curie) temperatures, $T_C \sim 0.6$ K (**1**) and 1.48 K (**2**), these "light atom" (PQN = 2) radicals appeared to violate Heisenberg's axiom, prompting Peter Day to draw a parallel with the comment of Dr. Johnson on seeing a dog walk on its hind legs: the surprise is not that it is done well, but that it is done at all.[5]
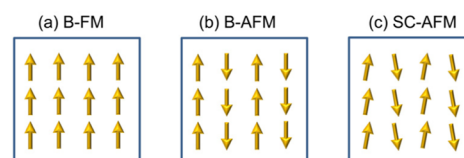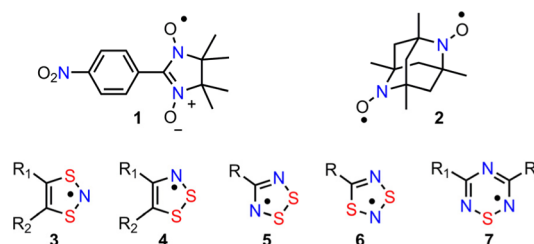
Following these landmark discoveries, the structures and magnetic properties of a wide range of light heteroatom (N, O) radicals, including nitroxyls, verdazyls, and triazinyls, were explored,[6] but little progress was made in terms of increasing FM ordering temperatures. The presence of bulky R-groups, required to impart stability to and prevent dimerization of the radical, coupled with the limited spatial extent of the singly occupied molecular orbital (SOMO), resulted in weak, low-dimensional magnetic interactions in the solid state that militated against high ordering temperatures. Moreover, in addition to their low T_C values, these early molecular radical magnets suffered from vanishingly small coercive fields H_c, by definition the reverse applied magnetic field required to demagnetize the sample. Questions therefore arose as to whether the concept of organic magnetism had reached its limits. Could ordering temperatures for radical-based ferromagnets be raised? Could radical-based magnetic materials with appreciable coercive fields be generated? The purpose of this Perspective is to respond to these questions.

LIGHT VERSUS HEAVY ATOMS

In principle, the intrinsic limitations of light heteroatom radicals as magnetic materials can be overcome by the incorporation of heavy (PQN ≥ 3) p-block elements (S, Se), which possess more spatially extensive valence orbitals capable of generating

stronger magnetic exchange interactions. Enhanced magnetic anisotropy, with the potential for larger coercive fields, might also be expected as a result of spin−orbit coupling (SOC) occasioned by the presence of the heavier heteroatom. However, the introduction of heavy atoms in spin-bearing sites comes at a cost, as the tendency for the resulting radicals to associate into spin-quenched, diamagnetic ($S = 0$) dimers is increased. Consistently, early solid-state structural work on thiazyl radicals **3−7**[7] revealed strongly associated dimers,[8] with radical pairs often bound by multicenter or "pancake" π-bonds.[9] Attempts to generate related phosphorus-centered radicals have met a similar fate,[10] and for selenium-based analogues of thiazyls the dimer binding energies are larger.[11] For some dithiazolyls **3** and **4**, however, association in the solid state is sufficiently weak that heat- and light-induced magnetostructural transitions between the dimer ($S = 0$) and a pair of radicals ($S = 1/2$) can be observed.[12,13] Suppression of low-temperature dimerization in dithiadiazolyls **5** was eventually achieved by judicious choice of R-group[8b] and was rewarded by the landmark discovery that the liberated spins can be magnetically active. The R = p-cyano-tetrafluorophenyl derivative orders as a spin-canted antiferromagnet (SC-AFM), in which adjacent spins are aligned almost antiparallel to one another but cant slightly so as to allow a net magnetic moment (Figure 1c). For this system, the ordering (Néel) temperature of $T_N = 36$ K,[14] remains to date the highest ever reported for a neutral radical. The p-nitro-tetrafluorophenyl analogue enters a B-FM phase with $T_C = 1.3$ K, in the same range as that found for light atom radicals.[15] In both cases, however, the resulting coercive field H_c is very small. Bulk AFM (B-AFM) order, where the spins are in a perfectly parallel alignment (Figure 1b), has also been reported (with $T_N = 11$ K) in a 1,3,2-dithiazolyl derivative **3**.[16]
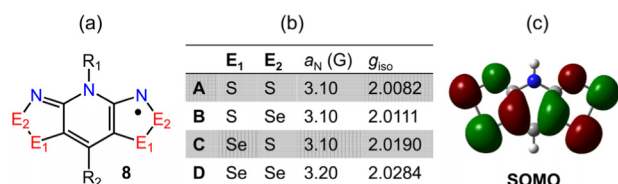

Figure 2. (a) Valence bond representation of a bisdithiazolyl **8**, with four S/Se variations **A−D**. (b) Isotropic a_N and g values for $R_1/R_2 =$ Et/Cl and (c) Kohn−Sham SOMO for a model **8A** ($R_1/R_2 =$ H) are also shown.

The drive to produce heavy atom radicals in which dimerization is suppressed more by electronic rather than steric factors, thus facilitating more three-dimensional (3D) electronic and magnetic networks, led to the design of resonance stabilized bisdithiazolyls **8** (Figure 2). In these systems, spin density is equally partitioned between two 1,2,3-dithiazole rings on either side of an N-alkylated pyridine bridge.[17,18] Synthetic strategies for site-specific incorporation of selenium were also developed,[19] thereby allowing the generation of families of isoelectronic radicals **8A−D**[20,21] and affording an ideal opportunity for the systematic study of magnetic and charge transport properties as a function of S/Se content.

Given the nodal properties of the a_2 symmetry SOMO of **8**, neither the beltline R_1/R_2 ligands nor the S/Se content have much effect on the molecular spin distribution, as witnessed by the invariance to ligand exchange of the EPR hyperfine coupling constant a_N to the "wing" nitrogens. However, the growth in the isotropic g-value with increasing Se content
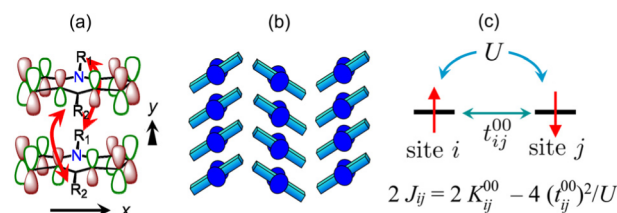

Figure 3. (a) Cofacial association of radicals **8A−D** is suppressed by spin delocalization and steric (R_1/R_1 and R_2/R_2) repulsion. Mutual slippage of the radicals along the local x and/or y directions (the latter runs into the page), with consequent changes in SOMO−SOMO overlap. (b) Herringbone packing of slipped π-stacks. (c) Two-site Hubbard model expressing site-to-site exchange coupling J_{ij} in terms of the onsite Coulomb potential U, and electron hopping (t_{ij}^{00}) and exchange (K_{ij}^{00}) integrals.

indicates an enhancement of SOC,[22] which sets the scale of magnetic anisotropy in the solid state. While the beltline R_1/R_2 ligands have little effect on molecular properties, their influence on crystal packing, and hence on solid-state electronic and magnetic structure, is profound. In most cases, the combination of steric protection offered by the substituents, coupled with increased spin delocalization, is sufficient to offset solid-state dimerization, even for Se-based radicals. Thus, in contrast to simple dithiadiazolyls **5** and their Se analogues, where pancake dimerization predominates,[8,9] the crystal structures of **8A−D** almost always consist of slipped π-stacks of radicals packed into herringbone arrays (Figure 3).[17] The structural diversity provided by different R_1/R_2 combinations, coupled with the fine-tuning of exchange interactions afforded by modification of S/Se content, has given rise to a wide range of magnetic phases, including B-FMs,[20] SC-AFMs,[23] metamagnets,[24] and spin ladders.[25]

■ MAGNEOSTRUCTURAL MAPPING

The packing patterns of radicals **8A−D** may be characterized by (i) the crystallographic space group and (ii) the specific direction and magnitude of relative slippage of adjacent radicals within the π-stacks. In order to quantify the latter parameters, it is convenient to define π-stack slippage (in Å) in terms of the local translation coordinates x and y, which describe the relative position of radicals when viewed perpendicular to their molecular planes, as shown in Figure 4. Thus, in a perfectly superimposed π-stack, where the radicals are eclipsed, the slippage coordinates would be $[x, y] = [0.0, 0.0]$. However, as noted above, steric repulsion between R_1/R_2 groups enforces finite slippage, the extent and direction of which varies with specific R_1/R_2 combination. Of particular interest are those radical families, defined by space group and slippage, where magnetic order is indicated by the appearance of a net moment, suggesting a B-FM or SC-AFM state. Representative members **8D** of two such families are shown in Figure 4. In the first, where $R_1/R_2 =$ Et/Cl (space group $P\bar{4}2_1m$), slippage occurs exclusively in the y direction, with $[x, y] = [0.0, 2.15]$. This tetragonal phase, found also for $R_1 =$ Et, $R_2 =$ F, Br, I, Me, hosts radicals displaying both B-FM and SC-AFM order.[20] For the second family, shown in Figure 4b, where $R_1/R_2 =$ Et/H (space group $P2_1/c$), SC-AFM order is common, and slippage along the x direction dominates, with $[x, y] = [3.3, 0.80]$.[23]

In each of the families of radicals **8A−D**, the specific pattern of order, when it is observed, is determined by the sign and magnitude of the intermolecular magnetic interactions which,
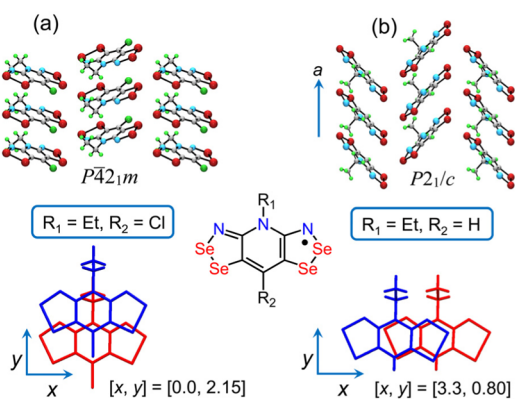
Figure 4. Herringbone arrays of **8D**, with (a) $R_1/R_2 =$ Et/Cl and (b) Et/H. Slippage of radicals along the π-stacks is defined in terms of translational coordinates x and y (in Å).

in the absence of spin−orbit effects (to be discussed later), may be in described in terms of the Heisenberg Hamiltonian shown in eq (1).

$$\mathcal{H} = -2J_{ij}\mathbf{S}_i \cdot \mathbf{S}_j \tag{1}$$

In this expression $J_{ij} > 0$ corresponds to a preference for FM alignment of spins on adjacent radical sites i,j, and $J_{ij} < 0$ denotes an AFM preference. From a theoretical perspective such interactions have been discussed in a variety of ways.[26,27] Here we use the two-site Hubbard model (Figure 3c),[28] including electron exchange between neighboring SOMOs, which affords the following expression for the value of J_{ij}.[29]

$$2J_{ij} = 2J_{ij}^{FM} + 2J_{ij}^{AFM} = 2K_{ij}^{00} - 4(t_{ij}^{00})^2/U \tag{2}$$

Of the various terms in eq (2), U is the onsite Coulomb potential, t_{ij}^{00} the intermolecular hopping integral, better known to chemists as a resonance integral, and K_{ij}^{00} the electron exchange integral (Figure 3c) . For the latter two terms the superscripted "00" indicates that the interaction is between neighboring SOMOs; the influence of other orbitals will be considered in later sections. In most cases the magnitude of J_{ij} is set by the AFM (−ve) virtual hopping term $-4 (t_{ij}^{00})^2/U$. However, with the inclusion of intersite electron exchange, which is generally small[30] but always +ve, the balance may be shifted in favor of a net FM interaction. The challenge is to design materials in which this condition prevails.

As a result of the strongly antibonding (nodal) nature of the SOMO (Figures 2 and 3), orbital overlap and hence t_{ij}^{00} and J_{ij}, are sensitive to solid-state packing, particularly the alignment (slippage) of neighboring radicals within in the same π-stack. Moreover, for such neighbors, the sign of the associated *intra*stack exchange interaction J_π is of critical importance for the emergence of B-FM and SC-AFM states. This is so because, for simple one- or two-sublattice ordered magnetic structures, symmetry restrictions require that a net magnetization may only appear when all crystallographic translation and inversion symmetries are maintained by the magnetic state. For this reason, B-FM and SC-AFM states in **8A−D** require spins within the same π-stack, which are related by translation, to be ferromagnetically aligned. Thus, J_π must be +ve, or sufficiently small that *inter*stack interactions dominate the magnetic order. Quantitative estimation of this parameter may be achieved using density functional theory (DFT) broken symmetry (BS) methods.[31] Results of this approach are illustrated in Figure 5,

which shows the variations in calculated J_π for sterically unhindered model radicals **8D** ($R_1/R_2 =$ H), as a function of translation along x and y (computed at the (U)B3LYP/6-31G(d,p) level).[21] The resulting two-dimensional (2D) energy surface shows regions of both FM (green) and AFM (blue) exchange, which may be related qualitatively to the expected pairwise overlap integral and hence t_{ij}^{00}. All four radicals **8A−D** produce qualitatively similar profiles, although the magnitude of J_π (be it +ve or −ve) is enhanced with increasing selenium content.
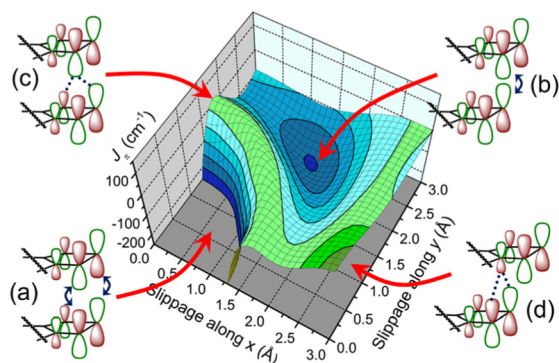

Figure 5. DFT-BS calculated J_π-energy surface for **8D** ($R_1/R_2 =$ H) as a function of π-stack slippage, with SOMO−SOMO overlap illustrated at key regions. (a) Strong −ve overlap near $[x, y] = [0, 0]$ and (b) +ve overlap near $[1.5, 2.0]$ gives rise to AFM (−ve J_π) exchange interactions, while weak (near-orthogonal) overlap around (c) $[x, y] = [0, 1.8]$ and (d) $[3.0, 0.0]$ is associated with FM (+ve) J_π values. Adapted with permission from ref 21. Copyright 2009 American Chemical Society.

Close inspection of Figure 5 allows the prediction of plate slippage regions conducive to either FM or AFM interactions along the π-stacks. For example, the deep AFM hole around $[x, y] = [0, 0]$ corresponds to the sterically unfavorable "pancake" overlap region, which would to lead to formation of a diamagnetic ($S = 0$) dimer, if found in nature. More subtle is the AFM well near $[1.5, 2.0]$, which may be loosely associated with strong Se1···Se2′ *intra*stack overlap between adjacent radicals. Experimentally, radicals falling into this regime, such as **8B,D** ($R_1/R_2 =$ Me/Cl, space group $P2_1/n$), with $[x, y] = [1.60, 1.54]$ and $[1.49, 1.64]$, respectively, indeed display strong AFM coupling along the π-stacks.[21] Consistently, these radicals do not show the onset of a canted moment down to $T = 2$ K, which would be symmetry forbidden. The two remaining models shown in Figure 5c,d correspond to slippage coordinates where FM exchange dominates within the π-stacks. The first, close to the (green) FM ridge that meets the $[0, y]$ plane near $y = 1.8$, corresponds to the tetragonal $P\bar{4}2_1m$ family illustrated in Figure 4a. The second, found near the point of maximum slippage along x (with y near 0), is shown in Figure 4b. In both cases, the occurrence of a positive J_π, required for B-FM and SC-AFM order, respectively, can be understood in terms of the classical orthogonal overlap condition[32] of neighboring SOMOs along the π-stacks, that is, where t_{ij}^{00} and hence $J_{ij}^{AFM} \sim 0$.

Provided ferromagnetic π-stack interactions, whether a material orders as a B-FM or SC-AFM is determined by the details of magnetic coupling *between* stacks, which may be remarkably sensitive to S/Se replacement. This observation is apparent in the magnetic properties of the four *isostructural* radicals **8A−D**
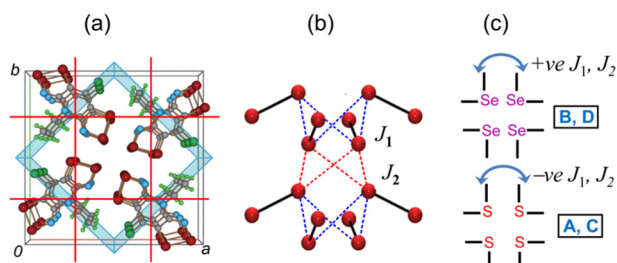
Figure 6. (a) Unit cell of **8D** (R_1/R_2 = Et/Cl), space group $P\bar{4}2_1m$, showing mirror planes and 2_1 axes. (b) Definition and (c) signs of interstack exchange interactions J_1 and J_2 in **8A–D** about the $\bar{4}$ points.

(R_1/R_2 = Et/Cl, space group $P\bar{4}2_1m$).[20] In the unit cell, four radicals encircle a $\bar{4}$-point, with each radical bisected by a local mirror plane, and adjacent radicals are related by 2_1 axes (Figure 6). While **8B** orders as a B-FM (like **8D**), with T_C = 12.8 K, **8C** adopts a SC-AFM phase with T_N = 14 K. Ordering has not been demonstrated for **8A** above 2 K, but the isostructural material with a R_2 = Br shows SC-AFM order with $T_N \sim$ 10 K.[33] The most important interstack interactions, labeled J_1 and J_2 in Figure 6b,c, occur between radicals related by 2_1 axes, and are mediated primarily via close E_2–E_2 contacts about the $\bar{4}$ points. On the basis of symmetry analysis, the SC-AFM states in **8A,C** (E_2 = S) most likely result from –ve J_1 and J_2 values, which enforce a checkerboard alternation of spin direction within the ab-plane. In this case, a canted moment parallel to the c-axis is allowed. In constast, in the ferromagnets **8B,D** (E_2 = Se), these two J-values are +ve on average, leading to the observed B-FM state.

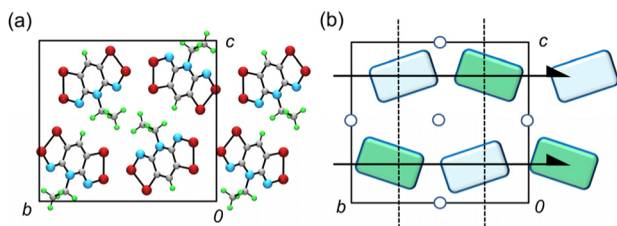**Figure 7.** (a) Unit cell of **8D** (R_1/R_2 = Et/H), space group $P2_1/c$, and (b) magnetic cell structure with associated symmetry operations (inversion centers and 2_1 axes). The two magnetic sublattices are distinguished by blue and green shading.

The role of interstack interactions in determining the pattern of magnetic order is also apparent in **8D** (R_1/R_2 = Et/H). Experimentally, this radical orders as a SC-AFM with T_N = 28 K; its isostructural analogue **8C** (R_1/R_2 = Et/H) behaves similarly, with T_N = 18 K.[23] The former displays a weakly AFM Weiss constant (Θ = –8 K), while the latter shows a net FM response at high temperatures, with Θ = +6 K. In these materials, symmetry restrictions related to the crystallographic inversion center allow for unambiguous determination of the magnetic structure (Figure 7), which implies FM *intra*stack and AFM *inter*stack interactions, as in the tetragonal materials. In this case, however, symmetry does not restrict the orientation of the observed canted moment, due to the low symmetry of the monoclinic space group.

■ CHEMICAL AND PHYSICAL PRESSURE

The observation of ordering, be it B-FM or SC-AFM, hinges on the existence of a net ferromagnetic response along the

π-stacks. For the tetragonal $P\bar{4}2_1m$ family of **8**, the DFT-BS structure map shown in Figure 5 suggests that intrastack exchange coupling J_π should be extremely sensitive to variations in slippage along the y direction (for x = 0). The orthogonal overlap condition where J_π is ferromagnetic spans a very narrow range, essentially where the FM "ridge" abuts the x = 0 "wall". Experimental support for this conclusion comes from the examination of the magnetic properties of a series of radicals of type **8B**, all belonging to the $P\bar{4}2_1m$ space group.[34] While the changes in R_1/R_2 are not sufficient to alter the space group, they are enough to induce subtle changes in slippage coordinates. The variations of these are illustrated in Figure 8, along with an assessment of the magnetic consequences, that is, the resulting change in J_π. While there is not an exact correspondence between the calculated and observed geometry expected for a FM response, one may conclude that slippage along y beyond that found for (i)–(iii) (R_1 = Et; R_2 = Cl, Br, Me) should eventually lead to AFM (–ve) J_π values and loss of B-FM or SC-AFM order. Consistently, the more highly slipped (iv), (v) (R_1 = CF_3CH_2, Pr; R_2 = Cl) show no evidence for either order down to 2 K.

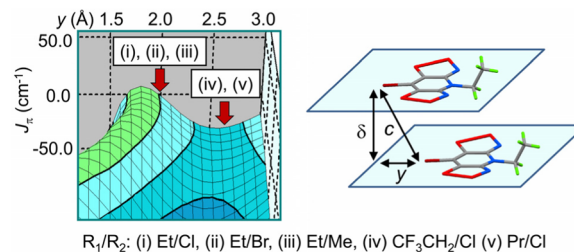R_1/R_2: (i) Et/Cl, (ii) Et/Br, (iii) Et/Me, (iv) CF_3CH_2/Cl (v) Pr/Cl

Figure 8. DFT-BS calculated J_π-energy surface for **8B** (R_1/R_2 = H) as a function π-stack slippage along the y direction, with observed y values of real systems. Radicals (i)–(iii) order as B-FMs, while (iv) and (v) do not order.

Exploration of the effect of changes in the ligands R_1/R_2 on the structure and magnetic response of a particular structure type represents an example of the use of "chemical pressure" to generate a magnetostructural response. An alternative approach, which allows for greater structural control, and hence more detailed insight, is to employ physical pressure.[35] By way of example we summarize in Figure 9 the results of high pressure (HP) crystallographic and magnetic measurements on **8D** (R_1/R_2 = Et/Cl).[20c,36] As expected, the application of pressure leads to the compression of the unit cell dimensions (Figure 9a), particularly the c-axis, which translates into a reduction of both the interlayer separation (δ, Figure 8) and the slippage of the π-stacks along the y direction. DFT-BS calculations of J_π as a function of pressure, using geometries obtained from the HP crystallographic data (Figure 9b), reveal a trend anticipated in Figure 9, that is, an initial increase in J_π as the FM "ridge" (where SOMO–SOMO overlap and t_{ij}^{00} is ~0) is traversed, followed by a rapid decrease as overlap and, hence, AFM interactions increase. The computational results provide a satisfying match with the pressure-induced variation in T_C (Figure 9b), that is, an initial rise to near 22 K at about 1 GPa, followed by a rapid decline, and probable loss of order. While the maxima in the J_π and T_C plots as a function of pressure do not coincide, the qualitative correspondence between the two profiles is appealing. These results highlight the fact that subtle increase or decrease in the degree of π-stack slippage, through chemical or physical pressure, respectively, can profoundly affect magnetic ordering.
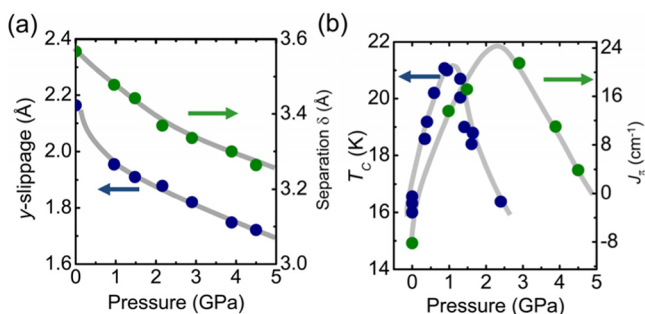
Figure 9. (a) Pressure-induced variations in plate separation along the π-stacks (δ) and slippage along the y direction for **8D** (R_1/R_2 = Et/Cl). (b) Changes in calculated J_π and experimental T_C as a function of applied pressure. Adapted with permission from ref 36. Copyright 2009 American Chemical Society.

■ HYSTERESIS AND ANISOTROPY

In previous sections, the enhancement of isotropic exchange interactions of resonance stabilized radicals **8A−D** served as a major motivation for pursuing the incorporation of selenium; it is the primary manifestation of the heavy atom effect. We now turn to the role selenium plays in mediating anisotropic exchange, as manifest in increased magnetic hysteresis and related phenomena. In contrast to $S > 1/2$ metal-based systems, where single-ion anisotropy may arise from local crystal field effects, Kramers' theorem forbids zero field magnetic anisotropy for isolated $S = 1/2$ radicals. In the solid state, coercivity and spin canting must therefore arise, in radicals, from interactions between spins, either through long-range dipolar effects, or anisotropic SOC corrections to the magnetic exchange. The former interaction depends on crystal morphology and microscopic structure and as such is largely independent of Se-incorporation. In contrast, the latter SOC effects may be enhanced directly by introduction of heavy elements into the molecular framework. In this regard, it is not surprising that early organic ferromagnets including nitroxyls,[4] thiazyls,[15] and doped fullerenes[37] displayed small coercive fields ($H_c < 10$ Oe). In these light atom materials, spin−orbit effects are relatively weak. By contrast, the first reported heavy atom (Se-based) organic ferromagnets **8B,D** (R_1/R_2 = Et/Cl) displayed significant hysteresis (Figure 10), with coercive fields (at 2K) of $H_c = 250$ and 1370 Oe, respectively, indicating significant anisotropy.[20b]

This magnetic anisotropy has been probed in both **8B,D** (R_1/R_2 = Et/Cl) through single crystal ferromagnetic resonance (FMR) measurements.[38] In FMR, the resonance conditions are sensitive *only* to the anisotropic component of the magnetic interactions, making the technique uniquely suited for studying such effects.[39] For tetragonal crystals, such as **8B,D** (R_1/R_2 = Et/Cl), the lowest order anisotropic contribution to the magnetic free energy is uniaxial and is characterized by an anisotropy field H_A, with an anisotropy energy $E_{aniso} = -1/2 H_A M \cos^2 \theta$. Here, θ is the polar angle measured with respect to the crystallographic c-axis, and M is the magnetization. By convention, for $H_A > 0$, magnetization is preferred along the c-axis (easy axis), while $H_A < 0$ refers to easy ab-plane anisotropy. At high frequency, the FMR resonant field of both radicals (Figure 11a) was found to vary in accord with the response predicted for easy c-axis anisotropy. As shown in Figure 11b, the magnitude of H_A was found to saturate, with decreasing temperature, toward values of 3.1 kOe for **8B** (at 4 K) and 8.8 kOe for **8D** (at 2 K),[38b] which may be compared with measured values for light atom ferromagnets,
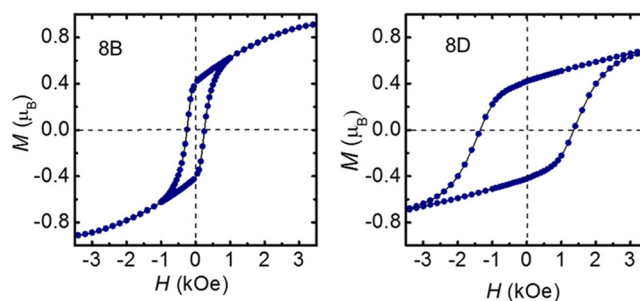

Figure 10. Magnetic hysteresis in **8B,D** (R_1/R_2 = Et/Cl) at T = 2K; H_c = 250 Oe (**8B**) and 1370 Oe (**8D**). Adapted with permission from ref 20b. Copyright 2008 American Chemical Society.

that is, 120 Oe for β-p-NPNN (at 0.4 K)[40] and 58 Oe for TDAE·C$_{60}$ (at 5 K).[41] While dipolar interactions provide an adequate explanation of the anisotropy in light-atom radicals,[42] the observed H_A (and H_c) is too large in **8B,D** (R_1/R_2 = Et/Cl) to originate from dipolar interactions. Dipolar interactions also fail to explain the scaling of H_A with Se content, suggesting H_A arises primarily from spin−orbit anisotropic exchange interactions, as described in the following section.
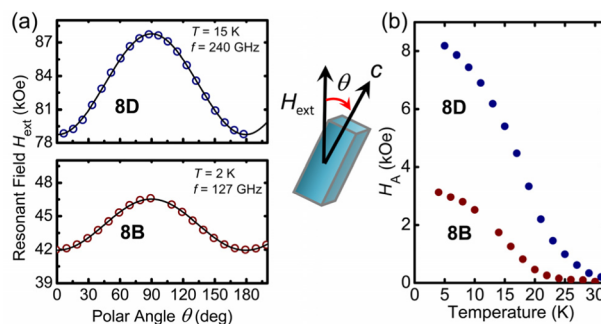

Figure 11. (a) Angular dependence of the resonant field H_{ext} for single crystals of **8B,D** (R_1/R_2 = Et/Cl) at f = 127 and 240 GHz. (b) Temperature dependence of H_A. Reprinted with permission from ref 38b. Copyright 2012 American Physical Society.

■ SPIN−ORBIT COUPLING

Coupling of spin **S** and orbital **L** momenta may be expressed, for isolated atomic ions, via the Hamiltonian $\mathcal{H}_{SO} = \lambda \mathbf{L} \cdot \mathbf{S}$, with a magnitude set by the empirical constant λ, which grows sharply with increasing atomic number (roughly as Z^4).[43] In molecular systems, however, the presence of multiatom and multielectron SOC contributions implies that $\mathcal{H}_{SO}$ cannot be expressed in terms of a single atomic parameter λ or operator **L**. Instead, one may introduce an effective one-electron molecular operator $\mathcal{L}$, such that $\mathcal{H}_{SO} = \mathcal{L} \cdot \mathbf{S}$, which may be computed in the spin−orbit mean field (SOMF) approximation.[44] At first order, the effect of this interaction in orbitally nondegenerate radicals is to mix filled and virtual orbitals to induce nonzero orbital angular momentum at the expense of the spin moment. The physical consequence of this mixing is that the spin/orbital composition of the observable magnetic moment becomes orientation dependent, which results in increased anisotropy in the g-tensors of isolated S- and Se-based radicals.[22] In the solid state, the interactions between composite spin−orbit moments are also rendered anisotropic and may be generally described by the Hamiltonian:

$$\mathcal{H} = -2J_{ij} \mathbf{S}_i \cdot \mathbf{S}_j + \mathbf{D}_{ij} \cdot \mathbf{S}_i \times \mathbf{S}_j + \mathbf{S}_i \cdot \mathbf{\Gamma}_{ij} \cdot \mathbf{S}_j \tag{3}$$

The first term in eq (3) represents the isotropic Heisenberg exchange interaction J_{ij} defined in eq (1) and described in terms of its ferromagnetic ($2K_{ij}$) and antiferromagnetic ($-4(t_{ij}^{00})^2/U$) components in eq (2). The second and third terms in eq (3) assess anisotropic exchange. Of these, the vector $\mathbf{D}_{ij}$ is the celebrated antisymmetric Dzyaloshinskii–Moriya (DM) interaction,[45] while the symmetric tensor $\mathbf{\Gamma}_{ij}$ represents the pseudo-dipolar (PD) interaction. Both DM and PD effects may contribute to H_A. The DM term prefers $\mathbf{S}_i$ and $\mathbf{S}_j$ to be canted with respect to one another, and lie in the plane normal to the $\mathbf{D}_{ij}$ vector, with $H_A \sim |\mathbf{D}_{ij}|^2/J_{ij}$. The PD term prefers $\mathbf{S}_i$ and $\mathbf{S}_j$ to be parallel (perpendicular) to the largest positive principal axes of the $\mathbf{\Gamma}_{ij}$ tensor for AFM (FM) aligned spins. The standard microscopic description of such terms is due to Moriya, who considered isolated $S = 1/2$ atomic centers and computed SOC corrections to the AFM exchange by means of eqs (4) and (5):

$$\mathbf{D}_{ij}^{AFM} = \frac{4i}{U}\{t_{ij}^{00}\mathbf{C}_{ji}^{00} - \mathbf{C}_{ij}^{00}t_{ji}^{00}\} \qquad (4)$$

$$\mathbf{\Gamma}_{ij}^{AFM} = \frac{4}{U}\{\mathbf{C}_{ij}^{00} \otimes \mathbf{C}_{ji}^{00} + \mathbf{C}_{ji}^{00} \otimes \mathbf{C}_{ij}^{00}\} \qquad (5)$$

where the SOMO–SOMO spin–orbit hopping term $\mathbf{C}_{ij}^{00}$ is a (pseudo)vector, with Cartesian components given in eq (6):

$$[\mathbf{C}_{ij}^{00}]_\mu = \frac{1}{2}\sum_a \left\{ \frac{\langle\phi_i^0|\mathcal{L}_i^\mu|\phi_i^a\rangle}{\epsilon_a - \epsilon_0}t_{ij}^{a0} + t_{ij}^{0a}\frac{\langle\phi_j^a|\mathcal{L}_j^\mu|\phi_j^0\rangle}{\epsilon_a - \epsilon_0} \right\} \qquad (6)$$

In the above $\mu \in \{x, y, z\}$, t_{ij}^{ab} is the hopping integral between orbital ϕ_i^a at radical site i and orbital ϕ_j^b at site j, the index a runs over all orbitals, and $a = 0$ refers to the SOMO. The orientation and magnitude of $\mathbf{C}_{ij}^{00}$ completely determines the character of the magnetic anisotropy. While Moriya's approach is equally valid for organic radicals, a conceptual disadvantage of writing $\mathbf{C}_{ij}^{00}$ in terms of the molecular operator $\mathcal{L}$ is that the energy scale for the interaction is no longer set by a single λ, complicating comparison of different molecular materials. Moreover, SOC may have varied effects on different orbitals, as discussed below. In order to address this complication, we introduce the orbital-dependent weighting functions shown in eqs (7) and (8), in which $|\epsilon_b - \epsilon_a| \leq \mathcal{E}$.

$$\mathcal{P}_\mu(a, \mathcal{E}) = \sum_{b \neq a} \left| \frac{\langle\phi_i^a|\mathcal{L}_i^\mu|\phi_i^b\rangle}{\epsilon_b - \epsilon_a} \right| \qquad (7)$$

$$\mathcal{P}_{tot}(a, \mathcal{E}) = \sum_{b \neq a} \sqrt{\sum_\mu \left(\left| \frac{\langle\phi_i^a|\mathcal{L}_i^\mu|\phi_i^b\rangle}{\epsilon_b - \epsilon_a} \right| \right)^2} \qquad (8)$$

Both functions quantify the degree of first-order spin–orbit mixing of orbital ϕ_i^a with all other orbitals lying within an energy window $\mathcal{E}$. The former function $\mathcal{P}_\mu$ for $\mu \in \{x, y, z\}$ describes the relative weight of SOC induced by the different Cartesian components of $\mathcal{L}$, which, for $a = 0$, is closely related to the orientation of $\mathbf{C}_{ij}^{00}$ and therefore the character of the anisotropic exchange. The latter function $\mathcal{P}_{tot}$ quantifies the total weight of mixing and is related to the overall scale of SOC, analogous to λ. Thus, for anisotropic exchange, $H_A \propto |\mathbf{C}_{ij}^{00}|^2$ and therefore should scale roughly as $[\mathcal{P}_{tot}(0, \mathcal{E})]^2$ in the limit of large $\mathcal{E}$. Values of $\mathcal{P}_{tot}(0, \mathcal{E})$ and $\mathcal{P}_\mu(0, \mathcal{E})$, computed at the
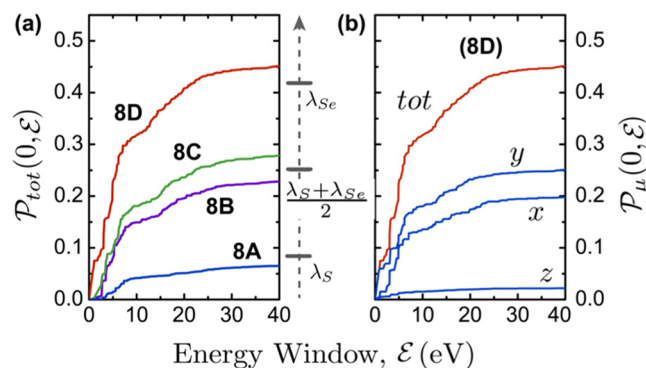

Figure 12. (a) Calculated weighting function $\mathcal{P}_{tot}(0, \mathcal{E})$ for **8A–D** (R_1/R_2 = Et/Cl) as a function of the width of the energy window $\mathcal{E}$. The limiting values of $\mathcal{P}_{tot}(0, \mathcal{E})$ appear in the same ratio as the average SOC constant for heavy (S, Se) atoms in the molecule. (b) Breakdown of Cartesian weights $\mathcal{P}_\mu(0, \mathcal{E})$ for **8D** showing a negligible component perpendicular to the molecular plane (z_i direction).

B3LYP/def2-SV(P) level using ORCA's SOC module,[46] are plotted in Figure 12 for **8A–D** (R_1/R_2 = Et/Cl).

The results indicate that the ratio of $\mathcal{P}_{tot}(0, \mathcal{E})$ between radicals **8A–D** converges toward a value determined by the average atomic λ of the chalcogen atoms[47] within the molecular framework. On this basis, one expects that H_A for **8B,D** should be roughly in the ratio $[(\lambda_S + \lambda_{Se})/2\lambda_{Se}]^2 = 0.36$. This estimate provides a satisfying correspondence with the ratio of the low-temperature H_A values obtained experimentally (∼0.35 from Figure 11b).

The origin of easy c-axis anisotropy in **8B,D** can be understood by examining the direction-dependent weighting functions $\mathcal{P}_\mu$, which are related to the orientation of $\mathbf{C}_{ij}^{00}$ (and therefore $\mathbf{D}_{ij}$ and $\mathbf{\Gamma}_{ij}$) for all neighboring pairs of radicals (Figure 12b). For this discussion we employ coordinates associated with each molecular site i analogous to the slippage coordinates introduced earlier; the x_i and y_i directions lie within the molecular plane, along the short and long axis of the molecule, respectively, while z_i lies normal to the molecular plane. In terms of such coordinates, the π-SOMO ϕ_i^0, is a linear combination of p_z orbitals, from which it follows that $\mathcal{L}_i^z|\phi_i^0\rangle \sim 0$ for the same reason that $\mathcal{L}_i^z|p_z\rangle = 0$ for isolated atoms. Thus, $\mathcal{P}_z(0, \mathcal{E})$ is nearly zero, implying the component of $\mathbf{C}_{ij}^{00}$ along the molecular normal at either site i (z_i) or at site j (z_j) will tend to be small. Put another way, for any two interacting sites, there is a strong tendency for $\mathbf{C}_{ij}^{00} \perp z_i, z_j$, which for **8B,D** implies that all $\mathbf{C}_{ij}^{00}$ will lie near the ab-plane. As this condition emerges only from the π-symmetry of the SOMO, it applies equally to all organic π-electron magnets and should serve as a general consideration in the analysis of other heavy atom organic materials, both neutral and charged.

To provide a quantitative estimate of the anisotropic exchange parameters, an ab-initio scheme suitable for organic systems has recently been introduced. When applied to **8D** (R_1/R_2 = Et/Cl), the computed $\mathbf{C}_{ij}^{00}$ was indeed found to lie near the ab-plane for all nearest-neighbor pairs. With both the DM and PD interactions preferring FM-aligned spins to be oriented perpendicular to $\mathbf{C}_{ij}^{00}$, the result is an easy c-axis. The sensitivity of SOC-mediated anisotropic exchange parameters to structural modification has also been probed in **8D** (R_1/R_2 = Et/Cl), by using physical pressure to drive π-stack slippage, as illustrated in Figure 9a, and high-field FMR spectroscopy to

monitor the resulting changes in H_A. Over the pressure range 0−2.2 GPa, H_A was found to increase monotonically, more than doubling to a value of 18.2 kOe at 2.2 GPa.[48] This pressure dependence is in marked contrast with the corresponding trend in T_C, which first rises and then begins to fall at pressures above 1 GPa, confirming that the isotropic and anisotropic interactions may scale differently with pressure. Ab-initio calculations correctly reproduced the pressure dependence of H_A and revealed that the enhancement is largely due to the increasing magnitude of *inter*stack hopping integrals upon compression of the crystal.

■ MULTIPLE ORBITALS

While isotropic and anisotropic exchange interactions in radicals **8A−D** have been well described in terms of a one-orbital Hubbard model, which includes *only* the SOMO explicitly, the importance of effects associated with other energetically nearby orbitals has recently been realized. These multi-orbital effects are relatively rare in radical-based magnetic materials,[49] but study of their propensity to generate ferromagnetic exchange by virtual hopping between the SOMO and empty orbitals has a long history, going back to work by Anderson[50] and Goodenough[51] on inorganic oxides. The ideas have since been applied to the design of ferromagnetic radical ion salts[52] and doped fullerenes.[53] In the context of bisdithiazolyl radicals, multi-orbital effects can be introduced by replacing the NR₁ unit of **8** with a carbonyl (CO) moiety, to afford the oxobenzene-bridged framework **9** shown in Figure 13.[54]
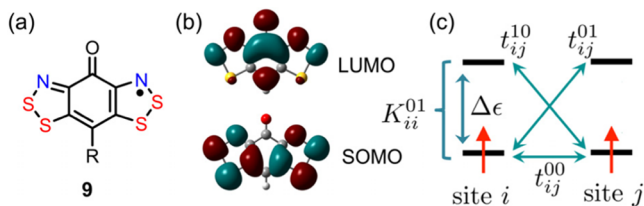

Figure 13. (a) VB bond representation of an oxobenzene-bridged bisdithiazolyl radical **9**. (b) Kohn−Sham a_2 SOMO and b_1 LUMO of **9** (R = H). (c) Four-orbital two-site orbital interaction diagram for two radicals **9** with a small SOMO−LUMO gap $\Delta\epsilon$. The SOMO−SOMO (t_{ij}^{00}) and SOMO−LUMO (t_{ij}^{10} and t_{ij}^{01}) hopping integrals and the SOMO−LUMO electron exchange integral K_{ii}^{01} are indicated.

While incorporation of the carbonyl group does not perturb the SOMO, mixing of the CO π^*-orbital results in a low-lying empty π-LUMO. The combination of a small HOMO−LUMO gap $\Delta\epsilon \sim 0.2$−0.4 eV with a large on-site SOMO−LUMO Hund's rule coupling K_{ii}^{01} requires modification of the FM exchange term in eq (2) to produce that shown in eq (9), in which the onsite Coulomb repulsion term V ($< U$) refers to two electrons in different orbitals.

$$2J_{ij}^{FM} = 2K_{ij}^{00} + 2\frac{(t_{ij}^{01})^2 + (t_{ij}^{10})^2}{(V + \Delta\epsilon)^2 - (K_{ii}^{01})^2}K_{ii}^{01} \qquad (9)$$

Structural studies on a range of oxobenzene-bridged radicals **9** (R = H, Me, Ph, F, Cl, Br, I)[55,56] reveal no evidence for herringbone style π-stacking, as observed for **8**. Instead, crystal packing is dominated by strong intermolecular S⋯O′ and S⋯N′ interactions which link adjacent radicals into coplanar ribbon-like arrays (Figure 14a). These "zig-zag" ribbons may then overlay to form slipped π-stacks, alternating ABABAB π-stacks and even brick-wall architectures (Figure 14b−d).

Magnetic studies on these materials have revealed several examples that display strong FM interactions along the π-stacks, with a pronounced tendency for SC-AFM order. When R = H, Ph, the radicals both order with $T_N \sim 4$ K and display strong ferromagnetic Weiss constants $\Theta = 16$ and 33 K, respectively.[55a,c] Consistent with the high Θ values, both materials undergo field-induced FM alignment under relatively small applied field. For the SC-AFMs with R = F, I (the latter as its EtCN solvate), the ordering temperatures are significantly higher ($T_N = 13$ and 35 K respectively),[55d,56] and these values, combined with the high symmetry and simplicity of the crystal structures, have allowed a detailed analysis of their magnetic structures.
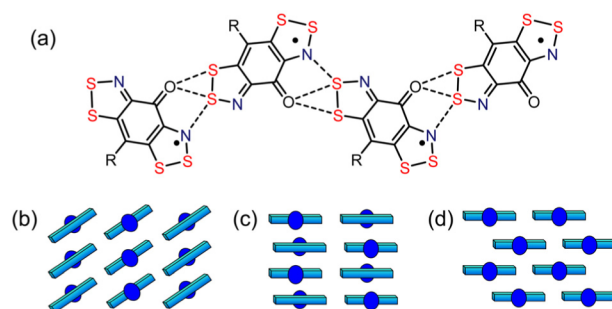

Figure 14. (a) Interlocking of radicals **9** into zigzag ribbon-like arrays, (b) slipped ribbon π-stacks, (c) alternating head-overtail π-stacks, and (d) brick wall π-stacks.

The crystal structures of radical **9** (R = F),[55d] space group $Cmc2_1$, and **9**·EtCN (R = I), space group $Pnma$,[56] are illustrated in Figure 15. Both consist of crystallographically coplanar arrays of radicals falling on a mirror plane. When R = F, the ribbon-like arrays illustrated in Figure 14a extend in both the b and c directions, to form 2D sheets at $x = 0, 0.5$ linked by a series of close, lateral S⋯O′ and S⋯N′ contacts. Neighboring radicals are related by C-centering or translation along b. In **9**·EtCN (R = I), each radical lies on a mirror plane normal to b at $y = 0.25, 0.75$ and is linked into ribbon-like arrays along the a-glide. The EtCN solvent molecules serve as buffers between adjacent ribbons and inhibit magnetic interactions between them. Due to the high symmetry of the $Cmc2_1$ and $Pnma$ space groups and the fact that radicals fall on a special position, the magnetic structure of each of these materials can be uniquely specified. For R = F, canting requires that all spins within the ab planes, which are related by translation (C-centering), belong to the same sublattice, that is, to be FM-aligned. Therefore, the only structure consistent with canting has ordering vector $(0, 0, 2\pi)$, with adjacent ab plane layers AFM-coupled, as shown in Figure 15. The canted moment is restricted to lie in the bc plane.[57] This structure requires strong ferromagnetic π-stack interactions within the brick walls, which ab-initio calculations confirm arise from multi-orbital exchange.

In the case of the centric structure **9**·EtCN (R = I), canting is possible only if sites related by either translation or inversion belong to the same magnetic sublattice. This condition is satisfied only for FM alignment of inversion-related spins on adjacent radicals in the same π-stack. Radicals related by the a-glide, coupled via lateral magnetic interactions, must be AFM-aligned, as shown in Figure 14, with individual moments lying in the ac plane. Numerical estimates of pairwise isotropic exchange energies are consistent with this pattern of magnetic order.[56]
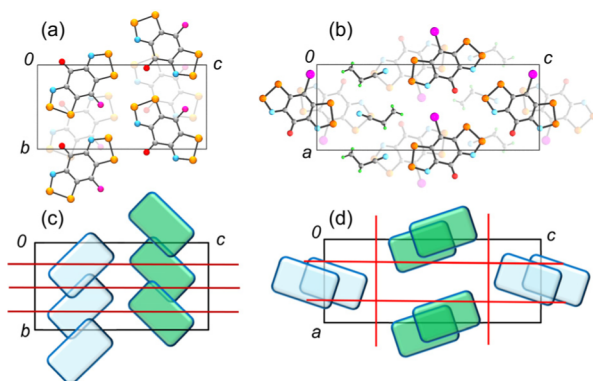
Figure 15. Unit cell drawings of (a) **9** (R = F), space group $Cmc2_1$, and (b) **9**·EtCN (R = I), space group $Pnma$, with cartoons of magnetic cells (c) and (d). The magnetic sublattices are distinguished by blue and green shading. The c-glide planes for R = F (c) and the n- and a-glide planes for R = I (d) are also shown (in red).
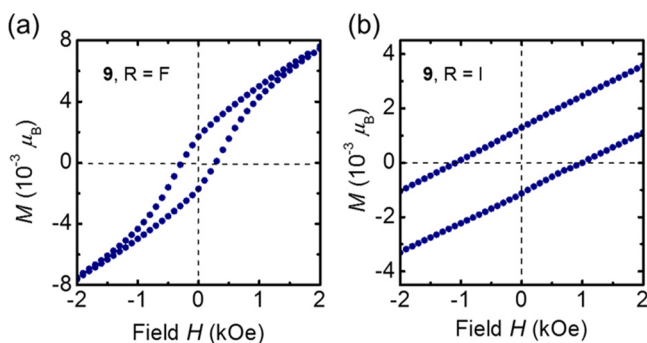

Figure 16. Magnetic hysteresis for (a) **9** (R = F) and (b) **9**·EtCN (R = I) at T = 2 K, where H_c = 290 and 1060 Oe, respectively. Adapted with permission from refs 55d and 56. Copyright 2012 and 2015 American Chemical Society.

In addition to promoting strong isotropic exchange interactions, multi-orbital effects also play an important role in determining the magnitude of the anisotropic exchange terms that influence spin canting and hysteresis. For the fluoro- and iodo-derivatives **9** (R = F, I) magnetic hysteresis measurements (Figure 16) reveal coercive fields H_c = 290 and 1060 Oe at T = 2 K, respectively, values comparable to those found in the Se-based ferromagnets **8B,D** (R_1/R_2 = Et/Cl). The anisotropy fields are, however, somewhat smaller. In the case of **9** (R = F) analysis of the powder antiferromagnetic resonance suggested easy plane anisotropy with $H_A \sim -200$ Oe,[57] while estimation of H_A from the spin-flop field H_{sf} in **9**·EtCN (R = I) indicated a value of $H_A \sim +630$ Oe.[56]

In **9** (R = F), where the R-group is a light atom, the relative role of dipolar interactions and SOC remains to be investigated, but in the latter case, SOC effects play a prominent role which may be ascribed the heavy iodine substituent. The observed magnetic anisotropy can only be understood by modification[58] of Moriya's standard description to include spin−orbit corrections to the multi-orbital FM exchange. Accordingly, and in order to describe multi-orbital anisotropic exchange, arising from SOC corrections to the second terms in eq (9), the following expressions, eqs (10) and (11), apply:

$$\mathbf{D}_{ij}^{FM} = -2i\left\{\frac{\mathbf{C}_{ij}^{01}t_{ji}^{10} - t_{ij}^{10}\mathbf{C}_{ji}^{01}}{(V + \Delta\epsilon)^2 - (K_{ii}^{01})^2}\right\}K_{ii}^{01} \tag{10}$$

$$\mathbf{\Gamma}_{ij}^{FM} = -2\left\{\frac{\mathbf{C}_{ij}^{01} \otimes \mathbf{C}_{ji}^{10} + \mathbf{C}_{ji}^{01} \otimes \mathbf{C}_{ij}^{10}}{(V + \Delta\epsilon)^2 - (K_{ii}^{01})^2}\right\}K_{ii}^{01} \tag{11}$$

These are distinguished from Moriya's conventional anisotropic exchange by the superscript "FM". The interorbital spin−orbit-mediated hopping $\mathbf{C}_{ij}^{01}$ is then given by eq 12:

$$[\mathbf{C}_{ij}^{01}]_\mu = \frac{1}{2}\sum_a\left\{\frac{\langle\phi_i^0|\mathcal{L}_i^\mu|\phi_i^a\rangle}{\epsilon_a - \epsilon_0}t_{ij}^{a1} + t_{ij}^{0a}\frac{\langle\phi_j^a|\mathcal{L}_j^\mu|\phi_j^1\rangle}{\epsilon_a - \epsilon_0 + V}\right\} \tag{12}$$

It is important to note from eq (12) that, in contrast to $\mathbf{C}_{ij}^{00}$ defined in eq (6), the value of $\mathbf{C}_{ij}^{01}$ depends on SOC effects in both the SOMO and the LUMO, through the first and second terms, respectively. As a result, while the magnitude of $\mathbf{C}_{ij}^{00}$ is related *only* to $\mathcal{P}_{tot}(0, \mathcal{E})$, the interorbital spin−orbit terms $\mathbf{C}_{ij}^{01}$ scale with *both* $\mathcal{P}_{tot}(0, \mathcal{E})$ and $\mathcal{P}_{tot}(1, \mathcal{E})$. To illustrate this point we show in Figure 17 the values of these two terms for **9** (R = F, Cl, Br, I), computed at the B3LYP/def2-SV(P) level, which reveal an important distinction between the behavior of the SOMO and LUMO. The a_2 SOMO contains a vertical nodal plane at the R-position (Figure 13), and consistently the SOC corrections are independent of both the R-group and the C=O moiety. For large $\mathcal{E}$, $\mathcal{P}_{tot}(0, \mathcal{E})$ converges to the same value in **9** and **8A**. By contrast, the b_1 LUMO, which possesses nonzero density at the R-position, shows spin−orbit effects that scale roughly with the spin−orbit constant λ_R, as quantified by $\mathcal{P}_{tot}(1, \mathcal{E})$.
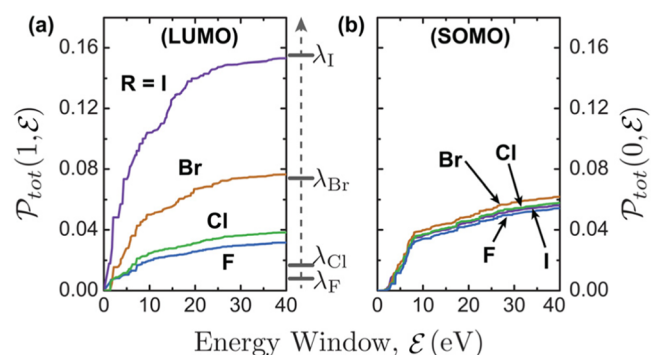

Figure 17. Calculated weighting functions $\mathcal{P}_{tot}(0, \mathcal{E})$ and $\mathcal{P}_{tot}(1, \mathcal{E})$ for the (a) LUMO and (b) SOMO of **9** (R = F, Cl, Br, I), as a function of the width of the energy window $\mathcal{E}$.

We conclude that in oxobenzene-bridged radicals **9**, multi-orbital anisotropic exchange may be selectively tuned by substitution at the R-position. This point is particularly well illustrated in **9**·EtCN (R = I), where both $\mathbf{D}_{ij}^{FM}$ and $\mathbf{\Gamma}_{ij}^{FM}$ are significantly enhanced by the heavy iodine substituent. By contrast, the symmetry of the SOMO and crystal conspires to restrict all conventional $\mathbf{D}_{ij}^{AFM}$ and $\mathbf{\Gamma}_{ij}^{AFM}$ interactions essentially to vanish. In this way, **9**·EtCN (R = I) represents not only a definitive example of multi-orbital anisotropic exchange but also demonstrates that the observation of magnetic anisotropy in highly symmetric crystal structures may be explained in terms of departures[58] from Moriya's conventional theory.

■ FUTURE PROSPECTS

In 2007, Stephen Blundell remarked, regarding radical-based magnets, that "few (radicals) are stable enough to be assembled

into crystalline structures and, even when that is possible, aligning these spins ferromagnetically is usually impossible".[59] The results summarized in this Perspective, which covers developments reported largely since that time, provide a more encouraging view of the opportunities available for such materials. It has been shown that significant improvement in the low ordering temperatures and small coercive fields which characterized early light atom (PQN < 3) radical magnets can be achieved by the incorporation of heavy heteroatoms. In materials such as **8A−D**, spin-pairing dimerization can be prevented by a combination of steric and electronic factors. These heavy atom (Se-based) organic magnets not only show strong isotropic exchange interactions but also display the effects (coercivity and spin-canting) of strong magnetic anisotropy arising from SOC. The recently introduced multi-orbital radical approach provides an alternative and potentially far-reaching means to enhance magnetic anisotropy, by incorporating heavy atoms into non-spin-bearing sites of a radical in which low-lying virtual orbitals are present. These virtual, heavy-atom-based orbitals can mix with the SOMO of a radical, thereby providing a means for the heavy atom to exert a spin−orbit effect while avoiding spin-pairing problems associated with the presence of spin density on a heavy atom.

Overall, the magnetic properties of the heavy atom radicals summarized here suggest a satisfying uniformity in the behavior of magnetic materials based on p-, d-, and f-electrons. Heisenberg was right, to generate strong exchange interactions all you need is PQN ≥ 3. Continued research into the magnetic properties of heavy p-block radicals may well provide a rich source of new spin−orbit related physics. For example, the possibility of realizing topologically nontrivial electronic or magnetic phases in organics and organometallics remains essentially unexplored.[60] Likewise the impact of SOC effects on spintronic devices based on organic semiconductors deserves further study. In these materials, anisotropic terms must be suppressed for long-lived spin coherence, while enhanced SOC is of importance for applications involving spin-transport, spin-charge conversion (the spin Hall effect), and other spin-dependent processes.[61] Engineering and tuning such properties in real systems requires a deep understanding of the relationship between spin−orbit parameters, molecular structure, and crystal architecture. As shown here, experimental and ab-initio probes of these relationships have already provided much insight.

From a practical perspective, the greatest challenges for the future, but also the greatest opportunities, lie in chemical synthesis, the demanding task of designing, building, and then crystallizing stable, main group heavy atom radicals in which dimerization is suppressed, and yet strong 3D magnetic exchange networks are preserved. While the neutral S−N and Se−N heterocycles described here have provided a rich array of magnetically active materials, exploration of π-delocalized inorganic ring systems based on other heavy p-block elements may eventually prove equally rewarding.[62] In this regard, an understanding of the structural properties of Te−N heterocycles is steadily emerging[63] and may yield breakthroughs. The pursuit of ferromagnetically coupled S−N (and Se−N) heterocyclic radical ion salts where multi-orbital effects apply also holds great potential.[52,64] Likewise recent reports of spin-delocalized radical cations of phosphorus-based heterocycles[65] provide encouragement for the pursuit of heavy group 15 neutral radicals. An alternative application of radicals, not developed in this Perspective, is as mediators of magnetic exchange

between coordinated metallic spin centers.[66] The use of heavy atom radicals in this role, as a means of enhancing magnetic anisotropy, has yet to be fully explored.

■ AUTHOR INFORMATION

Corresponding Author
*oakley@uwaterloo.ca

Notes
The authors declare no competing financial interest.

■ REFERENCES

(1) For useful introductions to the field of magnetism, see (a) Coey, J. M. D. *Magnetism and Magnetic Materials*; Cambridge University Press: Cambridge, 2010. (b) Jiles, D. *Introduction to Magnetism and Magnetic Materials*; Chapman and Hall: London, 1991. (c) Blundell, S. J. *Magnetism, a Very Short Introduction*; Oxford University Press: Oxford, 2012.

(2) In Heisenberg's words, "Die Hauptquantenzahl der für den Magnetismus verant wortlichen Electronen muß $n \geq 3$ sein." See: Heisenberg, W. *Z. Phys.* **1928**, *49*, 619.

(3) (a) Tamura, M.; Nakazawa, Y.; Shiomi, D.; Nozawa, K.; Hosokoshi, Y.; Ishikawa, M.; Takahashi, M.; Kinoshita, M. *Chem. Phys. Lett.* **1991**, *186*, 401. (b) Kinoshita, M. *Philos. Trans. R. Soc. London A* **1999**, *357*, 2855.

(4) Chiarelli, R.; Novak, M. A.; Rassat, A.; Tholence, J. L. *Nature* **1993**, *363*, 147.

(5) Day, P. *Nature* **1993**, *363*, 113.

(6) (a) Miller, J. S. *Adv. Mater.* **2002**, *14*, 1105. (b) Miller, J. S. *Mater. Today* **2014**, *16*, 224. (c) Lahti, P. M. In *Carbon Based Magnetism: An Overview of the Magnetism of Metal Free Carbon-based Compounds and Materials*; Makarova, T., Palacio, F., Eds.; Elsevier Science: Amsterdam, 2006; Chapter 2. (d) Kinoshita, M. In *π-Electron Magnetism: From Molecules to Magnetic Materials*; Veciana, J., Arcon, D., Eds.; Springer-Verlag: Berlin, 2001; Chapter 1. (e) Ratera, I.; Veciana, J. *Chem. Soc. Rev.* **2012**, *41*, 303. (f) Lahti, P. *Adv. Phys. Org. Chem.* **2011**, *45*, 93. (g) Karoui, H.; Le Moigne, F.; Ouari, O.; Tordo, P. In *Stable Radicals: Fundamentals and Applied Aspects of Odd-Electron Compounds*; Hicks, R. G., Ed.; John Wiley & Sons, Ltd.: Wiltshire, U.K., 2010; pp 173−229.

(7) (a) Rawson, J. M.; Alberola, A.; Whalley, A. *J. Mater. Chem.* **2006**, *16*, 2560. (b) Hicks, R. G. In *Stable Radicals: Fundamentals and Applied Aspects of Odd-Electron Compounds*; Hicks, R. G., Ed.; John Wiley & Sons, Ltd.: Wiltshire, U.K., 2010; pp 317−380. (c) Boeré, R. T.; Roemmele, T. L. *Comprehensive. Inorganic Chemistry II*; Elsevier Ltd.: Amsterdam, 2013; Vol. *1*, p 375. (d) Shuvaev, K. V.; Passmore, J. *Coord. Chem. Rev.* **2013**, *257*, 1067.

(8) (a) Oakley, R. T. *Prog. Inorg. Chem.* **1988**, *36*, 299. (b) Rawson, J. M.; Banister, A. J.; Lavender, I. *Adv. Heterocycl. Chem.* **1995**, *62*, 137. (c) Haynes, D. A. *CrystEngComm* **2011**, *13*, 4793.

(9) (a) Beneberu, H. Z.; Tianza, Y.-H.; Kertesz, M. *Phys. Chem. Chem. Phys.* **2012**, *14*, 10713. (b) Preuss, K. E. *Polyhedron* **2014**, *79*, 1. (c) Cui, Z.; Lischka, H.; Beneberu, H. Z.; Kertesz, M. *J. Am. Chem. Soc.* **2014**, *136*, 12958.

(10) Edge, R.; Less, R. J.; McInnes, E. J. L.; Müther, K.; Naseri, V.; Rawson, J. M.; Wright, D. S. *Chem. Commun.* **2009**, 1691.

(11) (a) Oakley, R. T.; Reed, R. W.; Cordes, A. W.; Craig, S. L.; Graham, S. B. *J. Am. Chem. Soc.* **1987**, *109*, 7745. (b) Cordes, A. W.; Haddon, R. C.; Oakley, R. T.; Schneemeyer, L. F.; Waszczak, J. A.;

Young, K. M.; Zimmerman, N. M. *J. Am. Chem. Soc.* **1991**, *113*, 582. (c) Cordes, A. W.; Haddon, R. C.; Hicks, R. G.; Oakley, R. T.; Palstra, T. T. M.; Schneemeyer, L. F.; Waszczak, J. V. *J. Am. Chem. Soc.* **1992**, *114*, 1729.

(12) (a) Barclay, T. M.; Cordes, A. W.; George, N. A.; Haddon, R. C.; Itkis, M. E.; Mashuta, M. S.; Oakley, R. T.; Patenaude, G. W.; Reed, R. W.; Richardson, J. F.; Zhang, H. *J. Am. Chem. Soc.* **1998**, *120*, 352. (b) Fujita, W.; Awaga, K. *Science* **1999**, *286*, 261. (c) McManus, G. D.; Rawson, J. M.; Feeder, N.; van Duijn, J.; McInnes, E. J. L.; Novoa, J. J.; Burriel, R.; Palacio, F.; Oliete, P. *J. Mater. Chem.* **2001**, *11*, 1992. (d) Brusso, J. L.; Clements, O. P.; Haddon, R. C.; Itkis, M. E.; Leitch, A. A.; Oakley, R. T.; Reed, R. W.; Richardson, J. F. *J. Am. Chem. Soc.* **2004**, *126*, 14692. (e) Vela, S.; Mota, F.; Deumal, M.; Suizu, R.; Shuku, Y.; Mizuno, A.; Awaga, K.; Shiga, M.; Novoa, J. J.; Ribas-Arino, J. *Nat. Commun.* **2014**, *5*, 4411. (f) Lekin, K.; Phan, H.; Winter, S. M.; Wong, J. W. L.; Leitch, A. A.; Laniel, D.; Yong, W.; Secco, R. A.; Tse, J. S.; Desgreniers, S.; Dube, P. A.; Shatruk, M.; Oakley, R. T. *J. Am. Chem. Soc.* **2014**, *136*, 8050. (g) Constantinides, C. P.; Berezin, A. A.; Zissimou, G. A.; Manoli, M.; Leitus, G. M.; Bendikov, M.; Probert, M. R.; Rawson, J. M.; Koutentis, P. A. *J. Am. Chem. Soc.* **2014**, *136*, 11906.

(13) (a) Hicks, R. G. *Nat. Chem.* **2011**, *3*, 189. (b) Rawson, J. M.; Hayward, J. J. In *Spin-Crossover Materials: Properties and Applications*; Halcrow, M. A., Ed.; J. Wiley & Sons: Chichester, U.K., 2013; p 235.

(14) Banister, A. J.; Bricklebank, N.; Lavender, I.; Rawson, J. M.; Gregory, C. I.; Tanner, B. K.; Clegg, W.; Elsegood, M. R. J.; Palacio, F. *Angew. Chem., Int. Ed. Engl.* **1996**, *35*, 2533.

(15) Alberola, A.; Less, R. J.; Pask, C. M.; Rawson, J. M.; Palacio, F.; Oliete, P.; Paulsen, C.; Yamaguchi, A.; Farley, R. D.; Murphy, D. M. *Angew. Chem., Int. Ed. Engl.* **2003**, *42*, 4782.

(16) Fujita, W.; Awaga, K.; Nakazawa, Y.; Saito, K.; Sorai, M. *Chem. Phys. Lett.* **2002**, *352*, 348.

(17) (a) Beer, L.; Brusso, J. L.; Cordes, A. W.; Haddon, R. C.; Itkis, M. E.; Kirschbaum, K.; MacGregor, D. S.; Oakley, R. T.; Pinkerton, A. A.; Reed, R. W. *J. Am. Chem. Soc.* **2002**, *124*, 9498. (b) Cordes, A. W.; Haddon, R. C.; Oakley, R. T. *Phosphorus, Sulfur, Silicon Relat. Elem.* **2004**, *179*, 673.

(18) (a) Beer, L.; Britten, J. F.; Brusso, J. L.; Cordes, A. W.; Haddon, R. C.; Itkis, M. E.; MacGregor, D. S.; Oakley, R. T.; Reed, R. W.; Robertson, C. M. *J. Am. Chem. Soc.* **2003**, *125*, 14394. (b) Beer, L.; Britten, J. F.; Clements, O. P.; Haddon, R. C.; Itkis, M. E.; Matkovich, K. M.; Oakley, R. T.; Reed, R. W. *Chem. Mater.* **2004**, *16*, 1564.

(19) Brusso, J. L.; Cvrkalj, K.; Leitch, A. A.; Oakley, R. T.; Reed, R. W.; Robertson, C. M. *J. Am. Chem. Soc.* **2006**, *128*, 15080.

(20) (a) Robertson, C. M.; Myles, D. J. T.; Leitch, A. A.; Reed, R. W.; Dooley, B. M.; Frank, N. L.; Dube, P. A.; Thompson, L. K.; Oakley, R. T.; Oakley. *J. Am. Chem. Soc.* **2007**, *129*, 12688. (b) Robertson, C. M.; Leitch, A. A.; Cvrkalj, K.; Reed, R. W.; Myles, D. J. T.; Dube, P. A.; Oakley, R. T. *J. Am. Chem. Soc.* **2008**, *130*, 8414. (c) Leitch, A. A.; Lekin, K.; Winter, S. M.; Downie, L. E.; Tsuruda, H.; Tse, J. S.; Mito, M.; Desgreniers, S.; Dube, P. A.; Zhang, S.; Liu, Q.; Jin, C.; Ohishi, Y.; Oakley, R. T. *J. Am. Chem. Soc.* **2011**, *133*, 6051.

(21) Leitch, A. A.; Yu, X.; Winter, S. M.; Secco, R. A.; Dube, P. A.; Oakley, R. T. *J. Am. Chem. Soc.* **2009**, *131*, 7112.

(22) Pivtsov, A. V.; Kulik, L. V.; Makarov, A. Y.; Blockhuys, F. *Phys. Chem. Chem. Phys.* **2011**, *13*, 3873.

(23) Leitch, A. A.; Brusso, J. L.; Cvrkalj, K.; Reed, R. W.; Robertson, C. M.; Dube, P. A.; Oakley, R. T. *Chem. Commun.* **2007**, 3368.

(24) Winter, S. M.; Cvrkalj, K.; Robertson, C. M.; Probert, M. R.; Dube, P. A.; Howard, J. A. K.; Oakley, R. T. *Chem. Commun.* **2009**, 7306.

(25) Lekin, K.; Wong, J. W. L.; Winter, S. M.; Mailman, A.; Dube, P. A.; Oakley, R. T. *Inorg. Chem.* **2013**, *52*, 2188.

(26) (a) Anderson, P. W. *Phys. Rev.* **1950**, *79*, 350. (b) Anderson, P. W. in *Theory of the Magnetic Interaction: Exchange in Insulators and Superconductors*; Turnbull, F., Seitz, F., Eds.; Academic Press: New York, 1963, Vol. 14; pp 99−214.

(27) (a) Kahn, O.; Briat, B. *J. Chem. Soc., Faraday Trans. 2* **1976**, *72*, 268. (b) Hay, P. J.; Thibeault, J. C.; Hoffmann, R. *J. Am. Chem. Soc.* **1975**, *97*, 488.

(28) Hubbard, J. *Proc. R. Soc. (London)* **1963**, *A276*, 238.

(29) (a) Calzado, C. J.; Cabrero, J.; Malrieu, J. P.; Caballol, R. *J. Chem. Phys.* **2002**, *116*, 2728. (b) Huang; Kertesz, M. *J. Phys. Chem. A* **2007**, *111*, 6304.

(30) (a) Vérot, M.; Rota, J.-P.; Kepenekian, M.; Le Guennica, B.; Robert, V. *Phys. Chem. Chem. Phys.* **2011**, *13*, 6657. (b) Domingo, A.; Vérot, M.; Mota, F.; de Graaf, C.; Novoa, J. J.; Robert, V. *Phys. Chem. Chem. Phys.* **2013**, *15*, 6982.

(31) (a) Noodleman, L. *J. Chem. Phys.* **1981**, *74*, 5737. (b) Noodleman, L.; Davidson, E. R. *Chem. Phys.* **1986**, *109*, 131. (c) Nagao, H.; Nishino, M.; Shigeta, Y.; Soda, T.; Kitagawa, Y.; Onishi, T.; Yoshioka, Y.; Yamaguchi, K. *Coord. Chem. Rev.* **2000**, *198*, 265. (d) Noodleman, L.; Norman, J. G. *J. Chem. Phys.* **1979**, *70*, 4903. (e) Deumal, M.; Bearpark, M. J.; Robb, M. A.; Pontillon, Y.; Novoa, J. J. *Chem.—Eur. J.* **2004**, *10*, 6422. (f) Deumal, M.; Rawson, J. M.; Goeta, A. E.; Howard, J. A. K.; Copley, R. C. B.; Robb, M. A.; Novoa, J. J. *Chem.—Eur. J.* **2010**, *16*, 2741.

(32) (a) Kahn, O.; Galy, J.; Journaux, Y.; Jaud, J.; Morgenstern-Badarau, I. *J. Am. Chem. Soc.* **1982**, *104*, 2165. (b) Kahn, O. *Molecular Magnetism*; VCH: New York, 1993. (c) Yoshizawat, K.; Hoffmann, R. *J. Am. Chem. Soc.* **1995**, *117*, 6921. (d) Verdaguer, M. *Polyhedron* **2001**, *20*, 1115.

(33) Winter, S. M. Ph.D. Thesis, University of Waterloo, 2014.

(34) Robertson, C. M.; Leitch, A. A.; Cvrkalj, K.; Myles, D. J. T.; Reed, R. W.; Dube, P. A.; Oakley, R. T. *J. Am. Chem. Soc.* **2008**, *130*, 14791.

(35) (a) Takeda, K.; Mito, M. In *Carbon-Based Magnetism*; Makarova, T., Palacio, F., Eds.; Elsevier: Amsterdam, 2005; pp 131−158. (b) Mito, M.; Kawae, T.; Hitaka, M.; Takeda, K.; Ishida, T.; Nogami, T. *Chem. Phys. Lett.* **2001**, *333*, 69. (c) Thomson, R. I.; Pask, C. M.; Lloyd, G. O.; Mito, M.; Rawson, J. M. *Chem.—Eur. J.* **2012**, *18*, 8629.

(36) Mito, M.; Komorida, Y.; Tsuruda, H.; Tse, J. S.; Desgreniers, S.; Ohishi, Y.; Leitch, A. A.; Cvrkalj, K.; Robertson, C. M.; Oakley, R. T. *J. Am. Chem. Soc.* **2009**, *131*, 16012.

(37) Suzuki, A.; Suzuki, T.; Whitehead, R. J.; Maruyama, Y. *Chem. Phys. Lett.* **1994**, *223*, 517.

(38) (a) Winter, S. M.; Datta, S.; Hill, S.; Oakley, R. T. *J. Am. Chem. Soc.* **2011**, *133*, 8126. (b) Winter, S. M.; Oakley, R. T.; Kovalev, A. E.; Hill, S. *Phys. Rev. B* **2012**, *85*, 094430.

(39) (a) Gurevich, A. G.; Melkov, G. A. *Magnetization Oscillations and Waves*; CRC Press: Boca Raton, FL, 1996. (b) Vonsovskii, S. *Ferromagnetic Resonance*; Pergamon Press: Oxford, 1968.

(40) Kambe, T.; Kajiyoshi, J.; Oshima, K.; Tamura, M.; Kinoshita, M. *Polyhedron* **2005**, *24*, 2468.

(41) Arcon, D.; Cevc, P.; Omerzu, A.; Blinc, R. *Phys. Rev. Lett.* **1998**, *80*, 1529.

(42) (a) Stanger, J.-L.; Andre, J.-J.; Turek, P.; Hosokoshi, Y.; Tamura, M.; Kinoshita, M.; Rey, P.; Cirujeda, J.; Veciana, J. *Phys. Rev. B* **1997**, *55*, 8398. (b) Kajiyoshi, K.-I.; Kambe, T.; Tamura, M.; Oshima, K. *J. Phys. Soc. Jpn.* **2006**, *75*, 074702.

(43) Dai, D.; Xiang, H.; Whangbo, M.-H. *J. Comput. Chem.* **2008**, *29*, 2187.

(44) (a) Hess, B. A.; Marian, C. M.; Wahlgren, U.; Gropen, O. *Chem. Phys. Lett.* **1996**, *251*, 365. (b) Neese, F. *J. Chem. Phys.* **2005**, *122*, 034107.

(45) (a) Moriya, T. *Phys. Rev.* **1960**, *120*, 91. (b) Dzyaloshinsky, I. *J. Phys. Chem. Solids* **1958**, *4*, 241.

(46) (a) Neese, F. *Wiley Interdiscip. Rev. Comput. Mol. Sci.* **2012**, *2*, 73. (b) Hess, B. A.; Marian, C. M.; Wahlgren, U.; Gropen, O. *Chem. Phys. Lett.* **1996**, *251*, 365.

(47) Blume, M.; Watson, R. E. *Proc. R. Soc. London, Ser. A* **1963**, *271*, 565.

(48) Thirunavukkuarasu, K.; Winter, S. M.; Beedle, C. C.; Kovalev, A. E.; Oakley, R. T.; Hill, S. *Phys. Rev. B* **2015**, *91*, 014412.

(49) (a) Kumai, R.; Matsushita, M. M.; Izuoka, A.; Sugawara, T. *J. Am. Chem. Soc.* **1994**, *116*, 4523. (b) Nakazaki, J.; Ishikawa, Y.; Izuoka, A.; Sugawara, T.; Kawada, Y. *Chem. Phys. Lett.* **2000**, *319*, 385.

(50) Anderson, P. W. *Phys. Rev.* **1959**, *115*, 2.

(51) (a) Goodenough, J. B. *J. Phys. Chem. Solids* **1958**, *6*, 287. (b) Goodenough, J. B. *Magnetism and the Chemical Bond*; Interscience-Wiley: New York, 1963.

(52) (a) Williams, K. A.; Nowak, M. J.; Dormann, E.; Wudl, F. *Synth. Met.* **1986**, *14*, 233. (b) Dormann, E.; Nowak, M. J.; Williams, K. A.; Angus, R. O.; Wudl, F. *J. Am. Chem. Soc.* **1987**, *109*, 2594. (c) Miller, J. S.; Epstein, A. J.; Reiff, W. M. *Chem. Rev.* **1988**, *88*, 201. (d) Fujita, W.; Awaga, K. *Chem. Phys. Lett.* **2004**, *388*, 186. (e) Fujita, W. *Dalton Trans.* **2015**, *44*, 903.

(53) (a) Allemand, P. M.; Khemani, K. C.; Koch, A.; Wudl, F.; Holczer, K.; Donovan, S.; Gruner, G.; Thompson, J. D. *Science* **1991**, *253*, 301. (b) .

(54) Wong, J. W. L.; Mailman, A.; Lekin, K.; Winter, S. M.; Yong, W.; Zhao, J.; Garimella, S. V.; Tse, J. S.; Secco, R. A.; Desgreniers, S.; Ohishi, Y.; Borondics, F.; Oakley, R. T. *J. Am. Chem. Soc.* **2014**, *136*, 1070.

(55) (a) Wong, J. W. L.; Mailman, A.; Winter, S. M.; Robertson, C. M.; Holmberg, R. J.; Murugesu, M.; Dube, P. A.; Oakley, R. T. *Chem. Commun.* **2014**, *50*, 785. (b) Yu, X.; Mailman, A.; Lekin, K.; Assoud, A.; Dube, P. A.; Oakley, R. T. *Cryst. Growth Des.* **2012**, *12*, 2485. (c) Yu, X.; Mailman, A.; Dube, P. A.; Assoud, A.; Oakley, R. T. *Chem. Commun.* **2011**, *47*, 4655. (d) Mailman, A.; Winter, S. M.; Yu, X.; Robertson, C. M.; Yong, W.; Tse, J. S.; Secco, R. A.; Liu, Z.; Dube, P. A.; Howard, J. A. K.; Oakley, R. T. *J. Am. Chem. Soc.* **2012**, *134*, 9886. (e) Yu, X.; Mailman, A.; Lekin, K.; Assoud, A.; Robertson, C. M.; Noll, B. C.; Campana, C. F.; Howard, J. A. K.; Dube, P. A.; Oakley, R. T. *J. Am. Chem. Soc.* **2012**, *134*, 2264.

(56) Mailman, A.; Winter, S. M.; Wong, J. W. L.; Robertson, C. M.; Assoud, A.; Dube, P. A.; Oakley, R. T. *J. Am. Chem. Soc.* **2015**, *137*, 1044.

(57) Winter, S. M.; Mailman, A.; Oakley, R. T.; Thirunavukkuarasu, K.; Hill, S.; Graf, D. E.; Tozer, S. W.; Tse, J. S.; Mito, M.; Yamaguchi, H. *Phys. Rev. B* **2014**, *89*, 214403.

(58) Yildirim, T.; Harris, A. B.; Aharony, A.; Entin-Wohlman, O. *Phys. Rev. B* **1995**, *52*, 10239.

(59) Blundell, S. J. *Contemp. Phys.* **2007**, *48*, 275.

(60) Wang, Z. F.; Liu, Z.; Liu, F. *Nat. Comms.* **2013**, *4*, 1471.

(61) (a) Boehme, C.; Lupton, J. M. *Nat. Nanotechnol.* **2013**, *8*, 612. (b) Ando, K.; Watanabe, S.; Mooser, S.; Saitoh, E.; Sirringhaus, H. *Nat. Mater.* **2013**, *12*, 622. (c) Watanabe, S.; Ando, K.; Kang, K.; Mooser, S.; Vaynzof, Y.; Kurebayashi, H.; Saitoh, E.; Sirringhaus, H. *Nat. Phys.* **2014**, *10*, 308. (d) Zheng, Y.; Wudl, F. *J. Mater. Chem. A* **2014**, *2*, 48.

(62) (a) Power, W. W. *Chem. Soc. Rev.* **2003**, *103*, 789. (b) Konu, J.; Chivers, T. In *Stable Radicals: Fundamentals and Applied Aspects of Odd-Electron Compounds*; Hicks, R. G., Ed.; John Wiley & Sons, Ltd.: Wiltshire, 2010; pp 381−404.

(63) (a) Cozzolino, A. F.; Elder, P. J. W.; Vargas-Baca, I. *Coord. Chem. Rev.* **2011**, *255*, 1426. (b) Cozzolino, A. F.; Vargas-Baca, I.; Mansour, S.; Mahmoudkhani, A. H. *J. Am. Chem. Soc.* **2005**, *127*, 3184. (c) Risto, M.; Assoud, A.; Winter, S. M.; Oilunkaniemi, R.; Laitinen, R. S.; Oakley, R. T. *Inorg. Chem.* **2008**, *47*, 10100. (d) Semenov, N. A.; Pushkarevsky, N. A.; Beckmann, J.; Finke, P.; Lork, E.; Mews, R.; Bagryanskaya, I. Y.; Gatilov, Y. V.; Konchenko, S. N.; Vasiliev, V. G.; Zibarev, A. V. *Eur. J. Inorg. Chem.* **2012**, 3693.

(64) Enoki, T.; Akira, M. *Chem. Rev.* **2004**, *104*, 5449.

(65) Su, Y.; Zheng, X.; Wang, X.; Zhang, X.; Sui, Y.; Wang, X. *J. Am. Chem. Soc.* **2014**, *136*, 6251.

(66) (a) Preuss, K. E. *Coord. Chem. Rev.* **2015**, 10.1016/j.ccr.2014.09.016. (b) Wu, J.; MacDonald, D. J.; Clérac, R.; Jeon, I.-R.; Jennings, M.; Lough, A. J.; Britten, J.; Robertson, C.; Dube, P. A.; Preuss, K. E. *Inorg. Chem.* **2012**, *51*, 3827. (c) Vela, S.; Sopena, A.; Ribas-Arino, J.; Novoa, J. J.; Deumal, M. *Chem.—Eur. J.* **2014**, *20*, 7083. (d) Fujita, W.; Awaga, K. *J. Am. Chem. Soc.* **2001**, *123*, 3601.